doi:10.1038/nature10283

Supplementary Methods

Study area: The Anaktuvuk River Fire scar is located on the North Slope of the Brooks Range, Alaska, USA (Supplementary Fig. 1), approximately 23 km NW of Toolik Field Station (68.5833 ^{o}N, 149.7167 ^{o}W). It is bounded on the east by the Nanushuk River and on the west by the Itkillik River, extending approximately 65 km from North to South (NW corner, 69.4273 ^{o}N , 151.0619 ^{o}W; NE corner, 69.4274 ^{o}N, 150.6980 ^{o}W; SW corner, 68.8637 ^{o}N, 150.5114 ^{o}W; SE corner, 68.9122 ^{o}N, 150.1311 ^{o}W; Supplementary Fig. 2). This region is underlain by permafrost. Mean annual temperature is approximately -10° C and mean annual precipitation is 30 cm. Long-term average growing season temperature (1971-2000) is about 10° C and tends to be somewhat warmer (1-2° C) at lower elevations, which range from 130 m asl at the north end of the burn to 450 m above sea level at the south end.

In July of 2007, the Anaktuvuk River Fire was started by lightning and sustained by growing season temperatures that were the warmest recorded over the 19 year record and precipitation that was only 25% of the long term average[33]. Warm and dry conditions were maintained by anomalous high pressure over the North Slope that appeared to be related to summer sea ice recession[34]. By the time snowfall extinguished the fire in early October, it had burned 1,039 km^2 of arctic tundra, doubling the cumulative area burned in this region over the past 50 years (Supplementary Table 1). This fire was an order of magnitude larger than the average fire size in the historic record for the North Slope (Supplementary Table 1) and remotely sensed indices of severity were substantially higher than for other recorded tundra burns[33].

Prior to the fire, 54% of the vegetated area within the burn perimeter was classified as upland moist acidic tundra (MAT; soil pH <5.5), 15% as moist non-acidic tundra (soil pH>5.5), and 30% as shrubland[35]. MAT is pan-Arctic in distribution and covers as much as 336 x 10^6 km^2 of the tundra biome[36]. We focused our study on MAT because of its widespread distribution and because the surviving growing points of the dominant plant species, Eriophorum vaginatum L., provided a benchmark of pre-fire soil organic matter depth and plant biomass. From this, we developed a method (described below) for estimating soil and plant organic matter consumption during fire using techniques similar to those described for boreal spruce forests[37]. Upland tundra soils contain, on average, 7,500 g C m^{-2} in the combustible organic horizon, but this varies substantially across the landscape, ranging from 100 to 63,000 g C m^{-2} (ref. 38). Mineral soils contain approximately 18,000 g C m^{-2} above the permafrost and a similar amount from the surface of the permafrost to 1 m depth[38]. Relict glacial ice wedges and lenses are common across the North Slope, as is high ice volume in near-surface permafrost[39].

Field sites: Twenty MAT sites within the burn were accessed via helicopter from either Umiat or Toolik Lake in July and August of 2008 (Supplementary Fig. 3). Burn severity was mapped using the differenced Normalized burn Ratio (dNBR) method[40] and sites 1-12 were randomly chosen to represent the range and frequency of dNBR values as described in Jones et al. (2009). The remaining sites, 13-20, were chosen randomly along hillslope transects from areas where collaborators had previously established eddy covariance towers and lake/stream monitoring.

To obtain empirical relationships between ecosystem structure and the element pools necessary for reconstruction of pre-fire soil C and N pools, 11 unburned MAT sites were also sampled

(Supplementary Fig. 3). Samples from one unburned site (ARF109) were held back from analyses for testing the reconstruction method. Three unburned sites were adventitiously encountered within the burn perimeter, an additional site was located near the 2007 Kuparuk Fire (69.2974 °N, 150.3221 °W), and seven others were systematically selected along the Dalton Highway. The latter sites were randomly selected from a GIS database that included all MAT areas along the Dalton within the elevation and climate range of the burn scar and were allocated to span the same elevations as the burn scar. All sites were >300 m from the road to minimize the effects of dust and other disturbances[41,42].

Tussock morphology: Our method for reconstructing pre-fire soil organic matter pools in burned sites was based on the relationship between the morphology of E. vaginatum tussocks and SOL depth. Tussocks are a columnar, caespitose growth form. At the top, many layers old leaf sheaths tightly clasp vertically growing short rhizomes (unthickened corms) that bear the tussock's living leaves and have apical and axillary growing points. These rhizomes are nestled in what we term the crown of the plant, a dense, compact mass of old leaf sheaths (upper arrow, Supplementary Fig. 4-A). The tussock's growing points are located 4.39 ± 0.26 cm (mean ± 1 SE, n=12 individual tussocks) below the crown's surface (lower arrow, Supplementary Fig. 4-A). The crown's dense, usually moist, mass of leaf sheaths resists burning and protects the growing points from heat damage during the fire, enabling rapid re-sprouting of leaves after fire (Supplementary Fig. 4-B). In unburned tundra, tussock crowns are located somewhat above the surface of the inter-tussock green moss (see below), and new leaf blades are further elevated above the moss layer (Supplementary Fig. 4-C). Beneath the crown, a deep, fibrous network of sheath-enclosed, proximal portions of corms tangles with a network of live and dead roots, to

form a column that extends down through the organic soil layer into the mineral soil. Eriophorum vaginatum is one of the few MAT species whose roots grow down into the mineral soil[43]. The tussock columns, topped with re-sprouting leaves, were a striking feature of the post-fire landscape (Supplementary Fig. 4-D).

Field sampling—unburned sites: We quantified the relationship between E. vaginatum crowns and SOL depth or biomass, and characterized SOL bulk density and element concentration across the 11 unburned sites. Along a 50 m transect in each site, we measured the depth of thaw and SOL at 5 m intervals (random point) and directly adjacent to the tussock nearest to the random point (n=10 random and 10 tussock points). We measured at both random and tussock points to determine whether the relationship between soil organic matter depth and tussock crowns was related to distance to tussock. Thaw depth was measured by inserting a metal rod into the soil until it hit ice or rock (differentiated by the sound and texture of the hit), marking the surface of the green moss on the rod, removing it, and measuring the distance from the tip to the mark with a meter stick. Soil organic layer depth was measured by slicing a square pit with a serrated knife, removing a monolith of organic soil, exposing the surface of the mineral soil, and measuring the distance from the surface of the green moss to mineral soil on two sides of the pit. The two depth measurements per pit were averaged to yield one SOL depth measurement per point.

At each point where SOL depth was measured, we used two meter sticks attached at a sliding right angle and fitted with a tubular spirit level to measure the depth of the green moss below a plane parallel to the crown of the nearest E. vaginatum tussock (Supplementary Fig. 5-A). Use

of the level ensured that the right angle was parallel to the crown and orthogonal to the ground. For the randomly located sample point, we also measured the distance to the nearest tussock using this apparatus. We measured the distance to, crown diameter of, and survivorship of the three next closest tussocks and used a nearest-neighbor method to estimate tussock density[44]. For each tussock, two crown diameter measurements were made (and averaged) at right angles by compressing the leaves and manually locating the sides of the crown.

To determine soil bulk density and element concentration, organic soil horizons were sampled volumetrically with a serrated knife. At 10 m intervals, a pit was dug and a 10 x 20 cm soil monolith was excised from the side of the pit, extending from the surface of the green moss to the surface of the mineral soil (roughly 5-30 cm depth depending on location). This monolith was wrapped in tinfoil to preserve structure, returned to the field station and frozen prior to shipping to the University of Florida (UF) for analyses of bulk density, moisture, C and N concentration, and C isotopes. All aboveground plant material attached to the surface of the soil monolith was included in the sampling. Tussocks were also harvested at 15 m intervals to develop allometric relationships between tussock diameter and combustible biomass (see below). Biomass was shaved from the live tussock with a serrated knife and returned to the field station, where it was dried at 70° C for 48 hours before weighing and shipping to UF for analyses of C and N concentration.

Field sampling—burned sites: Measurements in burned sites were similar to those in unburned sites except that measurements were made on the surface of the residual burned organic layer

rather than the surface of the green moss (Supplementary Fig. 5-B), and tussock leaves were not sampled.

Laboratory analyses: Approximately 155 soil monoliths comprising ~1000 individual 5 cm increment soil samples were collected in total from the 20 burned and 11 unburned sites. In the lab, each monolith was bisected depth-wise with an electric carving knife. One half of the monolith was processed for radiocarbon measurements, as described below, and re-frozen for archival purposes. In the remaining half, green moss and dwarf shrubs were sliced off and the remainder of the core was sliced into 5 cm depth intervals with the last sample of variable depth depending on the location of the organic/mineral interface. Samples were homogenized by hand and coarse organic materials (>2.5 cm twigs and roots) and rocks were removed. Coarse and fine organic fractions were weighed wet, dried at 70° C for 48 hours to determine dry matter content, then ground on a Wiley mill with a 40 mm sieve. Carbon and N content was measured on a Costech Elemental Analyzer (Costech Analytical, Los Angeles, California, USA) calibrated with the NIST peach leaves standard (SRM 1547, National Institute of Standards and Technology, Gaithersburg, MD, USA). The volume of each monolith layer was calculated as depth times area minus the volume of rocks. Bulk density, C or N pools were calculated for both fine and coarse organic fractions.

We used radiocarbon dating of the organic soil surface remaining post-fire to examine whether the fire burned into ancient and likely irreplaceable soil C pools. Because the moss and organic soil layer accumulates vertically through time, the radiocarbon values of the remaining organic matter can provide some indication of how long it took to accumulate the organic matter above it

that was consumed during the fire. Two cores were selected from each of ten sites randomly selected from the 20 sampling sites and sliced into 1 cm depth increments. Moss macrofossils were removed from the top layer under a dissecting scope. Cellulose was extracted from the macrofossils[45] and the sample was converted to graphite at 650°C with an iron catalyst in a hydrogen atmosphere[46]. Our primary standard for ^{14}C analysis was NIST oxalic acid II (SRM 4990C, National Institute of Standards and Technology). For a secondary standard, we used IAEA-C6 sucrose standard (International Atomic Energy Agency, Vienna, Austria). Our blank was anthracite coal cleaned with a standard acid–base–acid treatment. All standards and blanks used for ^{14}C measurements were combusted and purified similarly to the samples. The ^{14}C content of the graphite was measured at the W. M Keck Carbon Cycle Accelerator Mass Spectrometry Laboratory at the University of California–Irvine.

Radiocarbon data are expressed as $\Delta\ ^{14}C$, which is the per mil (‰) difference between the $^{14}C/^{12}C$ ratio of the sample and an international standard. Each sample was corrected for the effects of mass-dependent isotope fractionation of ^{14}C values by correcting to a constant $\delta^{13}C$ value of -25 ‰ and normalized to sample-specific measured $\delta^{13}C$ values. $\delta^{13}C$ was measured prior to graphitizing the CO_2 at the University of Florida on a Delta XL isotope ratio mass spectrometer with a gas bench peripheral (Thermo Scientific, Waltham, MA), using a -10.46 ‰ PDB CO_2 standard from Oztech (Stafford, Arizona, USA). In some circumstances, radiocarbon values during the bomb period (1950 to present) do not return unequivocal date estimates because of the shape of the atmospheric bomb curve (Figure 1; ref. 47). In a subset of those cases, we also analyzed the second, deeper 1 cm increment of organic soil for radiocarbon in order to determine the appropriate location of the surface date relative to the bomb peak. All

samples had radiocarbon values above zero, so samples where the deeper segment was more enriched in radiocarbon then the surface segment were assigned to the ascending slope of the bomb peak (<1966), while samples where the deeper segment was more depleted than the surface segment were assigned to the descending slope (>1966).

Estimating pre- and post-fire organic matter pools and losses: Post-fire SOL C and N pools were calculated for each 5 cm depth increment of residual organic soil at each sampling point in the burned sites (Supplementary Table 2). Total residual soil profile depth of randomly located samples did not differ significantly from those measured adjacent to tussocks (paired-t=0.68, P=0.50, n=20 sites), so we used the randomly located sampling points for our calculations. Coarse and fine fraction pools were summed at each depth and depths were summed across the profile to estimate total SOL element pools on a per site basis. The only aboveground vegetation encountered was from re-sprouting individuals and thus was not included in the post-fire pool estimates. No green moss was found on the surface of any of the soil monoliths, emphasizing the homogeneity of surface burning in this fire.

Estimates of depth and element loss on a per site basis required reconstruction of pre-fire depth or element pools for each site. Reconstruction of pre-fire SOL depth in burned sites was based on the observation that E. vaginatum crowns tended to be at the same height as the SOL surface in unburned tundra. We used the transect measurements in the unburned reference sites (described above) to derive a predictive relationship between tussock crown height (TCH) above the mineral soil surface and SOL depth, here the distance between the top of the green moss and the mineral soil surface. Soil organic layer depth measurements did not differ detectably

between random and tussock points (paired-t=0.21, P=0.70, n=10 sites), so we again used the randomly located points for our analyses. Tussock crown height was highly positively correlated with SOL depth (least squares regression, SOL depth (cm) = -1.126 + ln (TCH) x 1.242, R^2=0.94, P<0.001, n=10 sites; Supplementary Fig. 6). Depths calculated with least squares regression differed from geometric mean regression by <1%, so we used the former with burned site TCH and residual soil depth measurements to estimate pre-fire SOL depth. Pre-fire SOL C and N pools were then calculated for each 5 cm depth increment using the average unburned bulk density and C or N concentration for that layer (Supplementary Table 2). Finally, combustion C or N losses from the SOL were calculated as the pre-fire C or N pool minus the post-fire C or N pool of any remaining organic soil.

Pre-fire biomass and element pools in green mosses, lichens, shrubs, forbs and graminoids were included in SOL loss estimates above because they were sampled quantitatively with the soil monoliths. To estimate pre-fire combustible tussock biomass (CTB), we first derived a predictive relationship between CTB and tussock diameter (TD) in the unburned sites (ln(CTB (dry g·tussock^{-1})) = 3.097 + TD^2 x 0.003, R^2=0.67, P<0.001, n=35 tussocks). We used this equation to predict combustible biomass per tussock in the burned sites, which was then multiplied by density to scale to biomass per m^2. The latter was multiplied by the average C (43 ± 1, mean ± SE) or N (0.78 ± 0.05) concentration of CTB across the unburned sites to calculate the combusted C or N pool for the tussocks. All statistical analyses were performed in SYSTAT 11.00.01 (SYSTAT software, Inc., Chicago, IL).

Literature Cited

33 Jones, B. M., Kolden, C. A., Jandt, R., Abatzoglou, J. T., Urban, F., and Arp, C. D., Fire behavior, weather, and burn severity of the 2007 Anaktuvuk river tundra fire, North Slope, Alaska. *Arctic Antarctic and Alpine Research* **41** (3), 309-316 (2009).

34 Hu, F. S., Higuera, P. E., Walsh, J. E., Chapman, W. L., Duffy, P. A., Brubaker, L. B. et al., Tundra burning in Alaska: Linkages to climatic change and sea ice retreat. *Journal of Geophysical Research-Biogeosciences* **115**, G04002 doi:10.1028/2009JG001270 (2010).

35 Auerbach, N. A., Walker, D. A., and Bockheim, J. G., Landcover map of the Kaparuk River basin, Alaska (Alaska Geobotany Center, Fairbanks, AK 1997).

36 Walker, D. A., Raynolds, M. K., Daniels, F. J. A., Einarsson, E., Elvebakk, A., Gould, W. A. et al., The circumpolar Arctic vegetation map. *Journal of Vegetation Science* **16** (3), 267-282 (2005).

37 Boby, L. A., Schuur, E. A. G., Mack, M. C., Johnstone, J. F., and Verbyla, D. L., Quantifying fire severity, carbon and nitrogen emissions in Alaska's boreal forests. *Ecological Applications* **26** (6), 1633-1647 (2010).

38 Ping, C. L., Michaelson, G. J., Jorgenson, M. T., Kimble, J. M., Epstein, H., Romanovsky, V. E. et al., High stocks of soil organic carbon in the North American Arctic region. *Nature Geoscience* **1** (9), 615-619 (2008).

39 Jorgenson, M. T. and Osterkamp, T. E., Response of boreal ecosystems to varying modes of permafrost degradation. *Canadian Journal of Forest Research-Revue Canadienne De Recherche Forestiere* **35** (9), 2100-2111 (2005).

40 Key, C. H. and Benson, N. C., in *Firemon: Fire effects monitoring and inventory system*, edited by D. C. Lutes, R. E. Keane, J. F. Caratti et al. (USDA Forest Service, Rocky Mountain Monitoring and Inventory System, Ogden, UT, 2005), pp. 25-36.

41 Walker, D. A. and Everett, K. R., Road dust and its environmental impact on Alaskan taiga and tundra. *Arctic and Alpine Research* **19**, 479-489 (1987).

42 Myers-Smith, I. H., Arnesen, B. K., Thompson, R. M., and Chapin, F. S., Cumulative impacts on Alaskan arctic tundra of a quarter century of road dust. *Ecoscience* **13** (4), 503-510 (2006).

43 Kummerow, J., Ellis, B. A., Kummerow, S., and Chapin, F. S., Iii, Spring growth of shoots and roots in shrubs of an Alaskan muskeg. *American Journal of Botany* **70**, 1509-1515 (1983).

44 West, P. W., *Tree and forest measurement*, 2nd ed. (Springer-Verlag, Heidleberg, 2009).

45 Gaudinski, J. B., Dawson, T. E., Quideau, S., Schuur, E. A. G., Roden, J. S., Trumbore, S. E. et al., Comparative analysis of cellulose preparation techniques for use with C-13, C-14, and O-18 isotopic measurements. *Analytical Chemistry* **77** (22), 7212-7224 (2005).

46 Vogel, J. S., Southon, J. R., and Nelson, D. E., Catalyst and binder effects in the use of filamentous graphite for AMS. *Nuclear Instruments & Methods in Physics Research Section B-Beam Interactions with Materials and Atoms* **29** (1-2), 50-56 (1987).

47 Levin, I. and Hesshaimer, V., Radiocarbon - a unique tracer of global carbon cycle dynamics. *Radiocarbon* **42** (1), 69-80 (2000).

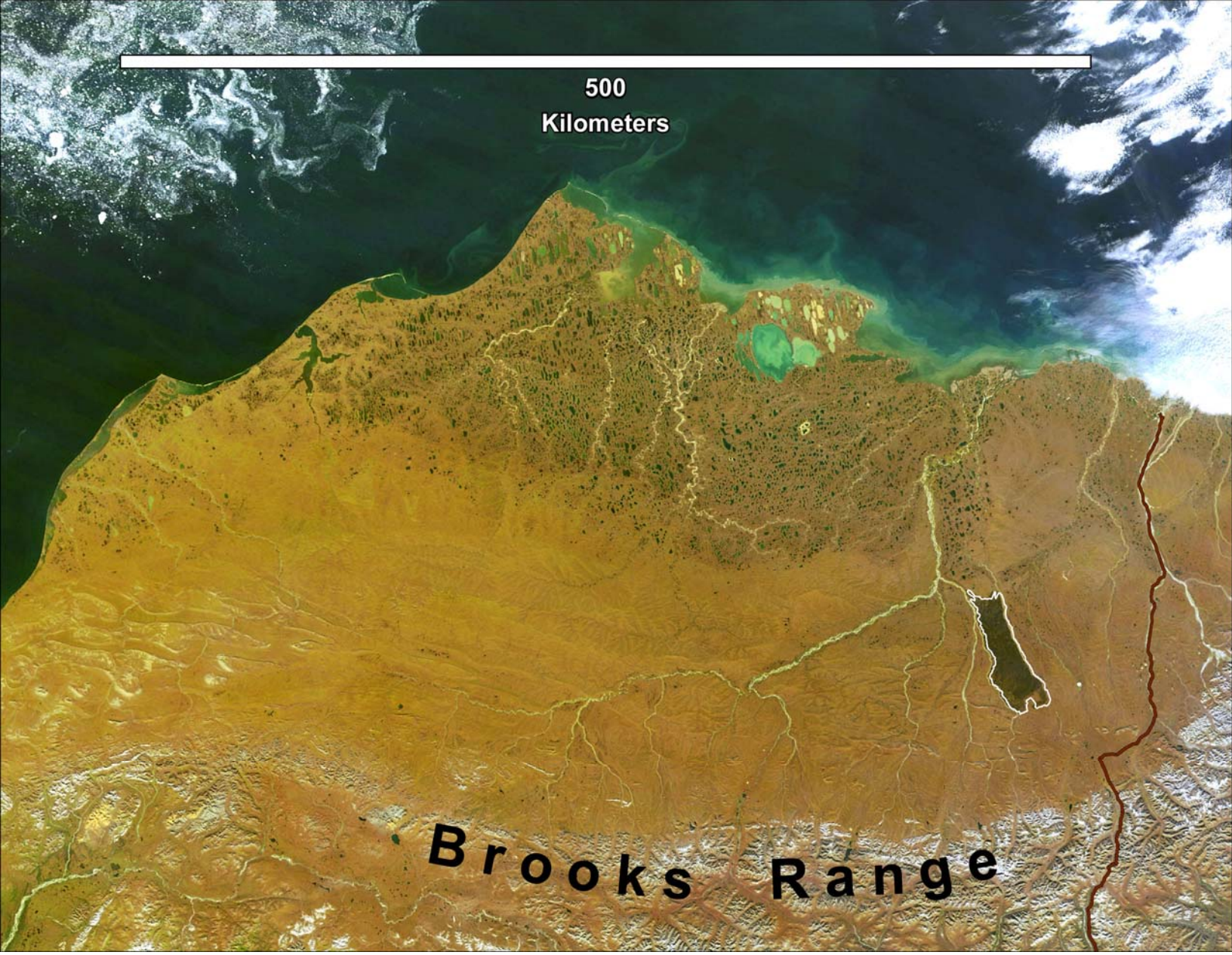

Supplementary Figure 1. NASA Terra MODIS image of the North Slope of the Brooks Range, USA, on 23 August 2008. The Anaktuvuk River fire, which burned in summer and fall of 2007, is outlined with a white boundary and the Dalton Highway is traced in red. This image is derived from exclusively public domain data.

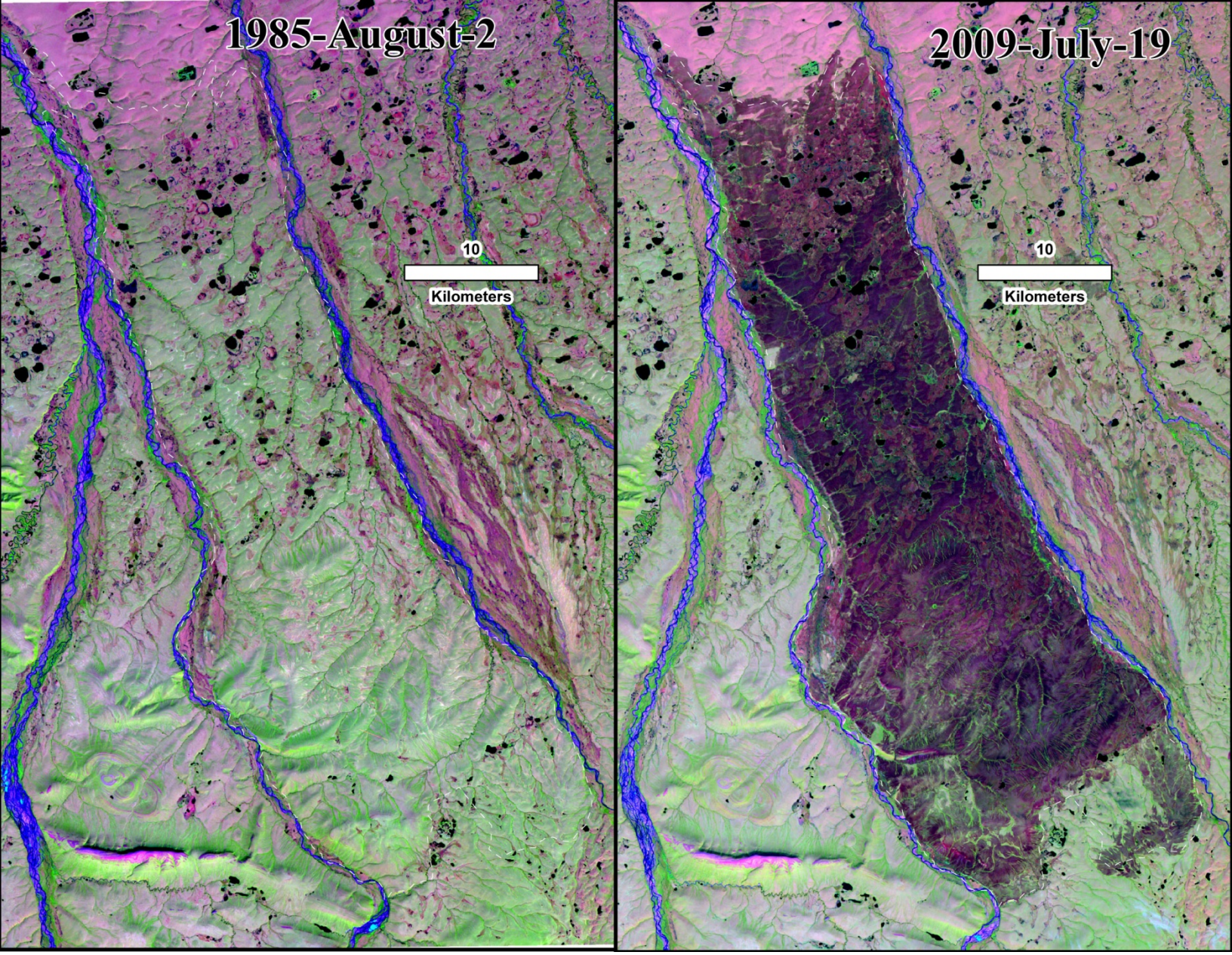

Supplementary Figure 2. Landsat TM images of the Anaktuvuk River Fire scar pre- and post-fire. The Nanushuk River on the east and the Itkillik River on the west acted as barriers to fire spread. The fire burned from upland tundra in the south end of the scar out onto the coastal plane, on the north end of the scar. This image is derived exclusively from public domain data.

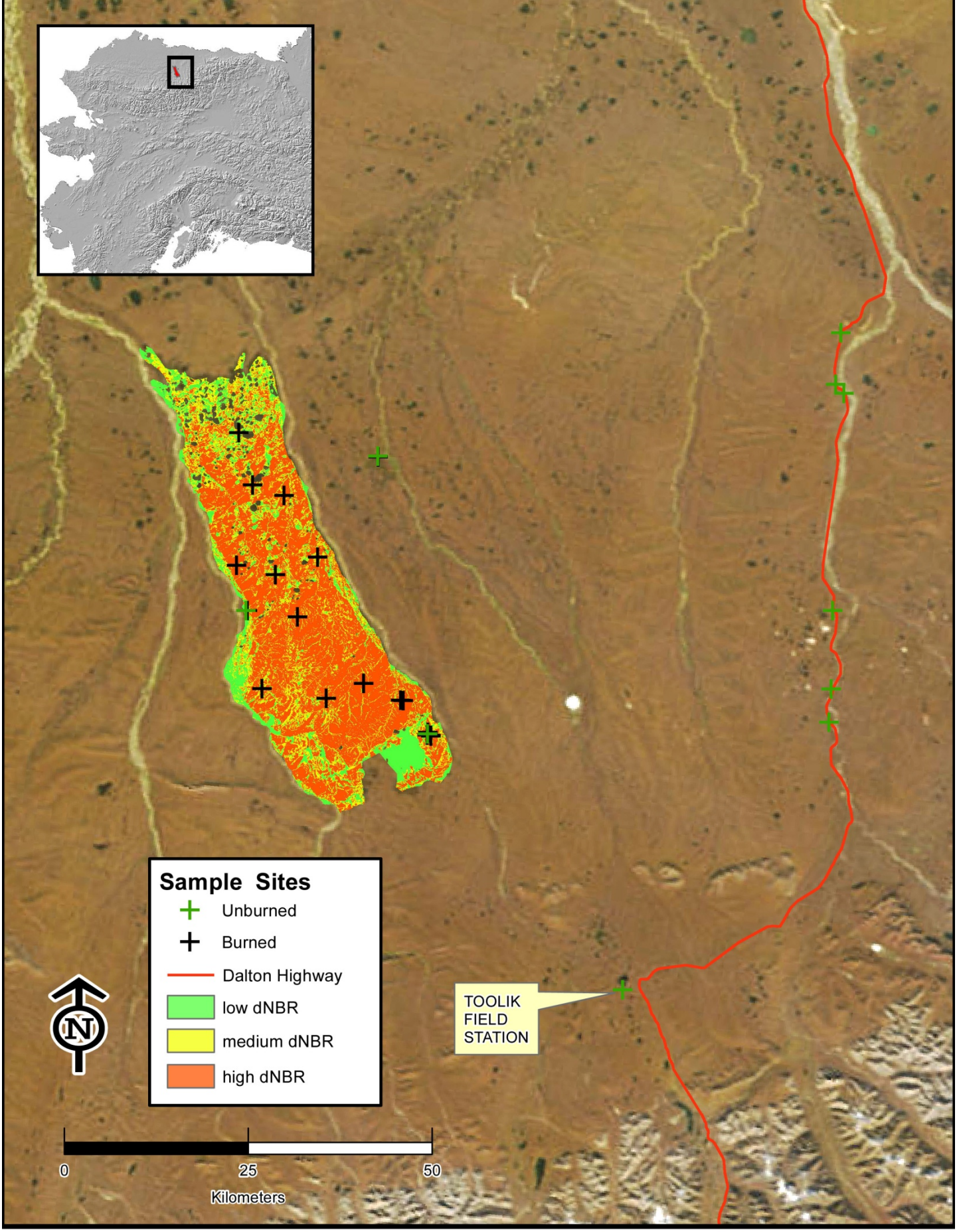

Supplementary Figure 3. Inset map shows the location of the Anaktuvuk River fire scar relative to the perimeter of the state of Alaska, UAS. Burn severity in the scare is indexed by dNBR (Jones et al. 2009). Sampling sites in burned (n=20) and unburned (n=10) tundra are indicated. Note that sites in the south end of the burn are closer together and symbols overlap.

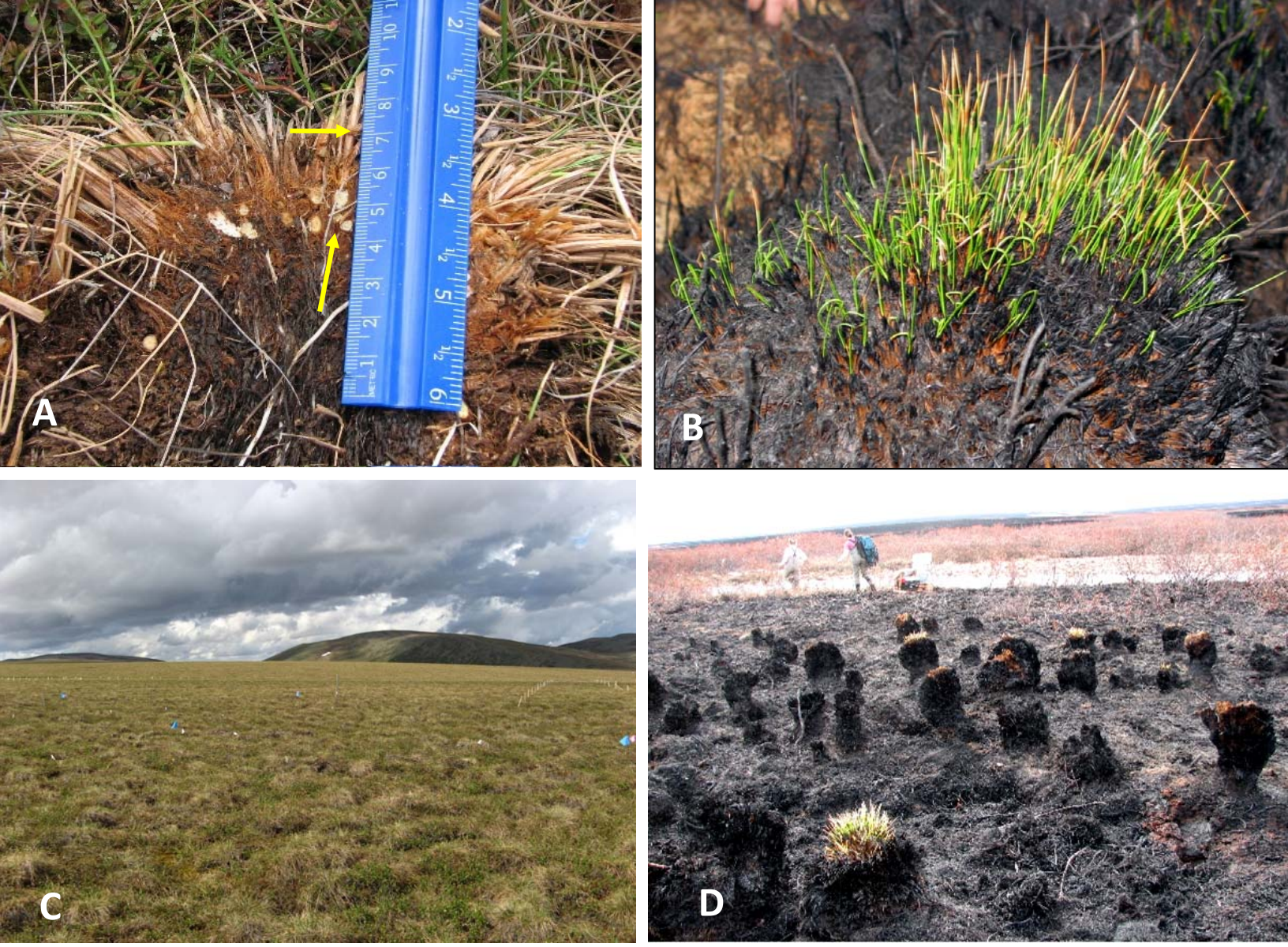

Supplementary Figure 4. *Eriophorum vaginatum* morphology and structure of moist acidic tundra on the North Slope of the Brooks Range, Alaska, USA. **A)** Bisected *E. vaginatum* tussock crown showing the location (lower arrow) or the plant's permanent stems (here termed corms) below the upper surface (upper arrow) of the dense mass of old leaf sheaths (here termed the tussock crown). **B)** Leaf blades extending out from tussock crowns in the spring after the fire. Their singed tips had been within the crown during the fire, but were close enough to its surface to become heat-injured. **C)** Surface of unburned, North Slope moist acidic tussock tundra showing current and recent years' leaf blades from crowns located slightly above the surface of the moss layer. **D)** Burned tussock tundra with characteristic columns of fibrous tussock roots plus crown and old, former corm tissue topped by resprouting leaves. *Photo credits: M. Syndonia Bret-Harte.*

A) Unburned moist acidic tundra

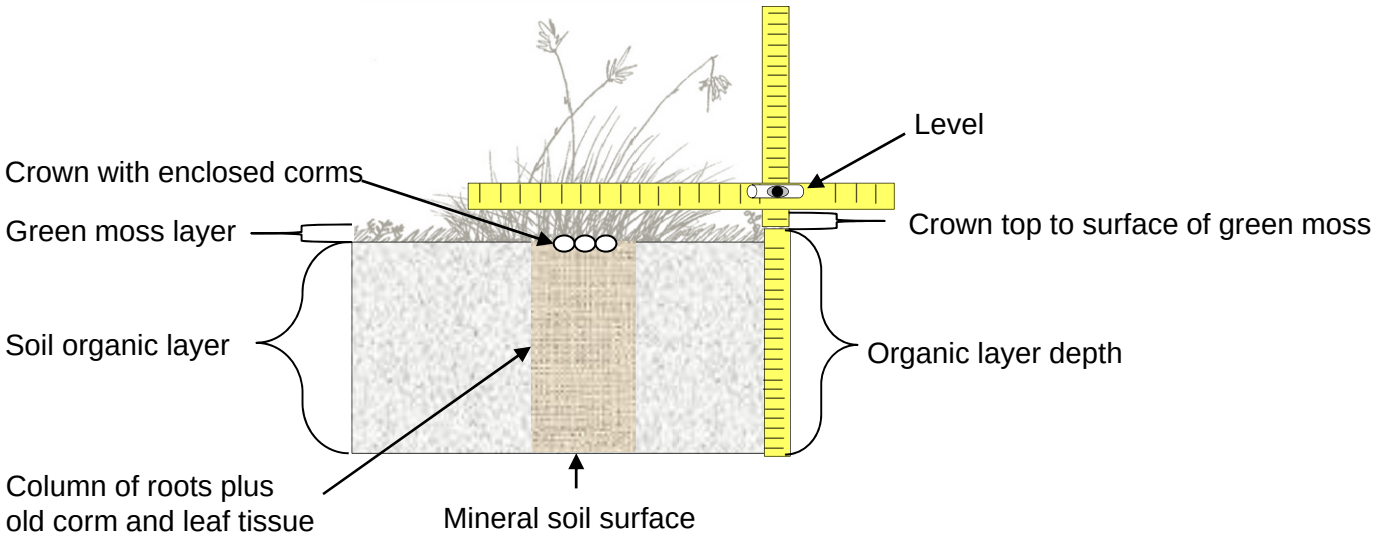

B) Burned moist acidic tundra

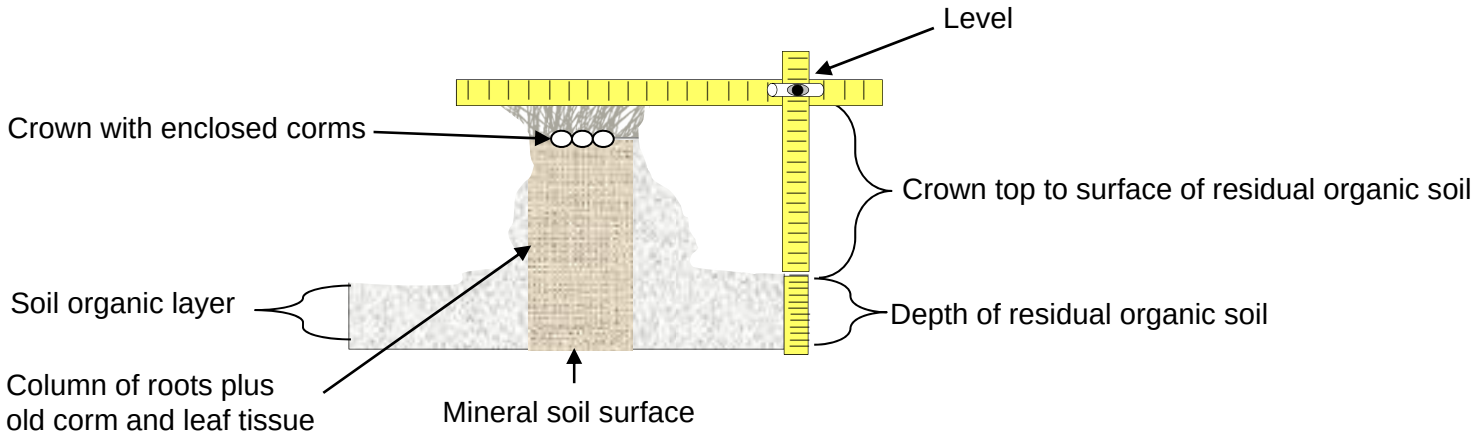

Supplementary Figure 5. Field measurements for reconstructing soil organic matter loss from fire. **A)** In unburned moist acidic tundra sites, the surfaces of the crowns of *Eriophorum vaginatum* tussocks were used as a reference point for the surface of the moss/organic soil layer. We quantified this by measuring the depth of a randomly located point on the green moss surface below a plane parallel to the crown of the closest *E. vaginatum* tussock. This plane was determined by leveling a pair of meter sticks that were attached at a sliding right angle. We also measured the depth of the soil organic later by digging a small soil pit, excising a monolith, and measuring the depth from the surface of the green moss to the surface of the mineral soil. In Figure 3, the crown to mineral soil depth is the sum of the crown top to surface of green moss distance and the organic layer depth. **B)** In burned sites, we made similar measurements except that the residual soil surface was used instead of the green moss surface.

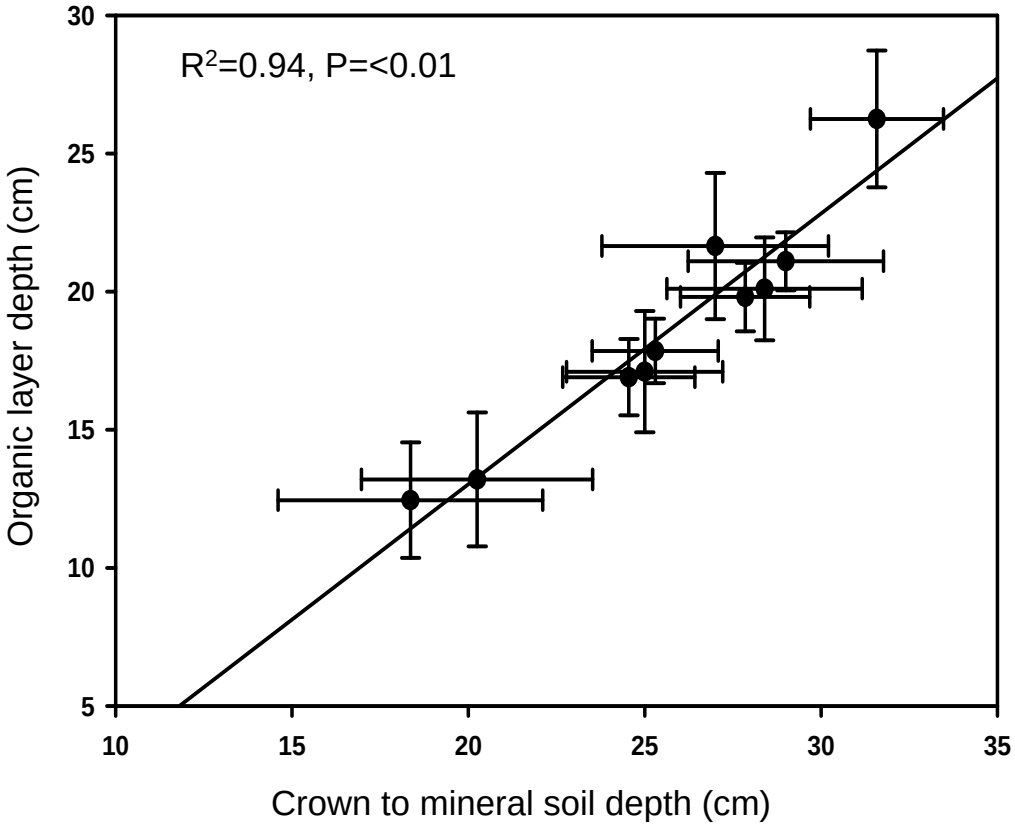

Supplementary Figure 6. Relationship between soil organic layer depth (moss surface to organic/mineral interface) and the depth from *Eriophorum vaginatum* crown tops to the mineral soil surface. Values are means of 10 randomly located measurements per site from 10 unburned sites sampled in or near the Anaktuvuk River Burn, or along the Dalton Highway, North Slope, Alaska.

Supplementary Table 1. Name, year and area burned of observed fires over 0.01 km^2 in size within the 188,448 km^2 North Slope region of Alaska, USA, over the last 50 years (source: Alaska Large Fire Database 2011: http://fire.ak.blm.gov/incinfo/aklgfire.php).

Fire Name	Year	Km^2
Anaktuvuk River Fire	2007	1039
DCKN190	1993	335
DCKN178	1993	68
AIN SSE 38	1977	47
Dead Horse	1976	28
731015	1987	16
Kavalina River	1999	15
Sagavanirktok	2007	13
Way Up North #2	1985	8
Kaparuk	2007	7
Tupikchak	1974	4
Kaparuk River	2001	3
Surprise Creek	2003	2
Baby Creek	2009	2
Kutchick River	2010	2
Niakogon Mountain	2010	1
Knifeblade Ridge	2010	<1
Kivalina	2009	<1
Maybe Creek	2010	<1

Supplementary Table 2. Mean (± 1 SE) characteristics of residual soil organic layer profiles in burned upland moist acidic tundra sites within the Anaktuvuk River Fire (2007) scar on the North Slope of the Brooks Range, Alaska USA. n=number of sites, where each site mean is an average of five profiles. ρ=bulk density. Note that only four sites had soils >15 cm deep after the fire.

			< 2.5mm diameter fraction					
Layer	Depth (cm)	N	ρ ($g \cdot cm^{-3}$)	%C	%N	C:N	C pool ($g \cdot C \cdot m^{-2}$)	N pool ($g \cdot N \cdot m^{-2}$)
Organic[a]	0-5	20	0.07	44.0	1.25	39	1,538	48.0
			(0.01)	(0.5)	(0.07)	(2)	(109)	(6.0)
	5-10	20	0.09	42.6	1.30	38	1,915	67.2
			(0.01)	(0.5)	(0.08)	(2)	(142)	(8.7)
	10-15	20	0.12	41.8	1.41	33	2,360	91.4
			(0.01)	(0.06)	(0.09)	(2)	(189)	(12.7)
	15-20	4	0.15	39.8	1.67	28	2,912	136.9
			(0.02)	(1.0)	(0.12)	(3)	(248)	(21.3)
	20-25	3	0.16	40.3	1.92	22	3,194	157.6
			(0.02)	(1.2	(0.14)	(2)	(410)	(26.7)
	25-30	3	0.20	34.8	1.54	23	3,544	163.4
			(0.04)	(3.0)	(0.18)	(2)	(749)	(48.5)
	30-35	1	0.25[b]	20.7	1.01	21	2,591	126.0
	35-40	1	0.26[b]	23.8	1.17	20	3,056	150.3

[a] Organic: soil organic layer was measured from the burned surface to the surface of the mineral soil (%C<20). Note that because the zero depth is the burned surface, depth increments here are not comparable to unburned soil depth increments.

[b] No standard error calculated because only one site had soils in this depth class.

Supplementary Table 2, continued.

		> 2.5mm diameter fraction					
Layer	Depth (cm)	P ($g \cdot cm^{-3}$)	%C	%N	C:N	C pool ($g \cdot C \cdot m^{-2}$)	N pool ($g \cdot N \cdot m^{-2}$)
Organic	0-5	0.005	50.3	0.8	70	58	0.9
		(0.001)	(0.3)	(0.01)	(2)	(13)	(0.02)
	5-10	0.005	49.7	0.8	67	49	0.8
		(0.001)	(0.4)	(0.01)	(3)	(7)	(0.1)
	10-15	0.014	49.1	0.9	64	252	10.5
		(0.011)	(0.8)	(0.10)	(5)	(213)	(10.1)
	15-20	0.004	50.1	1.1	50	44	1.0
		(0.001)	(0.6)	(0.1)	(4)	(13)	(0.3)
	20-25[c]	0.003	44.5	0.9	50	34	0.6
		(0.002)	(2.5)	(0.2)	(12)	(17)	(0.3)

[c] No material in this size class was encountered below 30 cm depth.

Supplementary Table 3. Mean (± 1 SE) combustible plant and soil organic layer profile characteristics of unburned upland moist acidic tundra (MAT) sites on the North Slope of the Brooks Range, Alaska USA. n=number of sites, where each site mean is an average of five profiles. ρ=bulk density. na=not applicable.

			< 2.5mm diameter fraction					
Layer	Depth (cm)	N	ρ ($g \cdot cm^{-3}$)	%C	%N	C:N	C pool ($g \cdot C \cdot m^{-2}$)	N pool ($g \cdot N \cdot m^{-2}$)
Tussocks[a]	>0	10	na	43.0 (1.0)	0.78 (0.05)	55 (1.32)	0.78 (0.05)	0.78 (0.05)
Other ag[b] biomass	>0	10	0.04 (0.001)	40.6 (1.2)	0.92 (0.04)	46 (2)	241 (22)	5.4 (0.5)
Organic[c]	0-5	10	0.07 (0.01)	38.2 (2.0)	0.93 (0.05)	44 (3)	1,256 (132)	33.4 (5.4)
	5-10	10	0.09 (0.01)	40.0 (1.1)	1.21 (0.09)	39 (3)	1,694 (141)	59.7 (10.2)
	10-15	10	0.13 (0.03)	39.2 (1.9)	1.44 (0.09)	31 (3)	2,377 (314)	103.3 (21.2)
	15-20	9	0.13 (0.02)	40.5 (1.2)	1.70 (0.14)	26 (2)	2,601 (334)	122.2 (23.3)
	20-25	8	0.15 (0.02)	37.7 (3.1)	1.71 (0.18)	23 (2)	2,794 (521)	138.3 (31.1)

25-30	2	0.18	39.8	2.18	19	3,434	197.7
		(0.04)	(3.5)	(0.01)	(3)	(417)	(34.1)
30-35	1	0.13[d]	41.5	2.21	20	2,721	146.4
35-40	1	0.20[d]	41.1	1.77	23	1,730	74.6

[a] Tussocks: biomass of Eriophorum vaginatum determined to be combustible by comparison of burned and unburned tussocks.

[b] Other ag biomass: all other vascular plant, green moss and lichen aboveground biomass harvested with the soil monoliths.

[c] Organic: soil organic horizon was designated as the surface of the brown moss to the surface of the mineral soil (% C <20).

[d] No standard error calculated because although n cores were processed for >2.5 mm dia fraction, only one sample had material in this size class.

Supplementary Table 3, continued.

		>2.5 mm diameter fraction					
Layer	Depth (cm)	ρ ($g \cdot cm^{-3}$)	%C	%N	C:N	C pool ($g \cdot C \cdot m^{-2}$)	N pool ($g \cdot N \cdot m^{-2}$)
Other ag[b] biomass	>0	0.0003 (0.0002)	50.3 (0.8)	0.54 (0.08)	99 (15)	4.9 (2.9)	0.06 (0.04)
Organic[c]	0-5	0.0024 (0.0006)	48.8 (0.6)	0.69 (0.05)	77 (6)	57.8 (13.0)	0.83 (0.21)
	5-10	0.0025 (0.0007)	48.8 (0.4)	0.86 (0.08)	65 (6)	62.1 (16.2)	1.05 (0.29)
	10-15	0.0011 (0.0005)	49.2 (0.6)	0.92 (0.10)	58 (7)	28.2 (11.4)	0.48 (0.20)
	15-20	0.0005 (0.0003)	45.6 (2.4)	1.14 (0.14)	46 (9)	11.7 (6.5)	0.29 (0.17)
	20-25	0.0001[d]	49.6	1.56	32	0.9	0.03
	25-30	0.0001 [d]	50.3	1.19	42	0.6	0.01
	30-35	0.0003 [d,e]	50.5	1.05	48	7.0	0.15

[e] No material in this size class was encountered below 35 cm depth.